Light-Scattering Study of Starlike Polymeric Micelles

Lena J. M. Vagberg,† Kathleen A. Cogan, and Alice P. Gast*

Department of Chemical Engineering, Stanford University, Stanford, California 94305-5025

Received June 19, 1990; Revised Manuscript Received September 24, 1990

ABSTRACT: We present light-scattering measurements confirming that poly(ethylene oxide)/polystyrene block copolymer micelles in cyclopentane undergo remarkable increases in aggregation number, from 17 to 77 upon saturation with water. This micellar molecular weight increase is responsible for the increase in the hydrodynamic radius we observed previously[1] and is accompanied by an increase in the radius of gyration. Micellar solutions saturated with water have insignificant concentrations of single chains and can be diluted at constant water activity. The second viral coefficient and the concentration dependence of the diffusion coefficient in these micelles reflect soft-sphere interactions. At low polymer concentrations, nonvirial changes in micellar size reflect further increases in aggregation number to the order of 100 chains/micelle. We interpret our scattering results in the context of a starlike micelle model. These structures comprise a solid core surrounded by a corona exhibiting the concentration profile expected for star-shaped polymers. We find that the starlike micelle describes the radius of gyration and hydrodynamic radius of our micelles quite well. This model only begins to fail as the aggregation number drops below 30 and the chains are no longer in semidilute conditions. We also present the ratio of hydrodynamic to gyration radius and find behavior spanning a region between Gaussian chain behavior and hard spheres.

Introduction

The similarity between block copolymers in selective solvents and surfactants was realized long ago[2,3] in the first studies showing block copolymer micelle formation. Many groups have studied micelle formation and emulsification in block copolymer solutions via a variety of analytical techniques.[4-6] Block copolymers dissolved in selective solvents are believed to form relatively monodisperse micelles above a critical micelle concentration. The number of chains per micelle, or aggregation number, is often quite large, on the order of 50 or more.[7,8] The expected structure as described in several recent reviews comprises a spherical core of insoluble blocks surrounded by a corona of solvated segments.[4,5,9]

We have recently discovered the sensitivity of block copolymer micelles to the presence of a second immiscible solvent compatible with the core.[1] We presented a dynamic light-scattering study showing the effect of water on the size of poly(ethylene oxide)/polystyrene diblock copolymers. We inferred that the addition of water to such a system augmented the aggregation number substantially, causing the observed increase in hydrodynamic size. In this paper we present the results of a static light-scattering study confirming the increase in apparent aggregation number and physical size.

Several groups have made the connection between block copolymer micelles and star-shaped polymers,[9,10] and one scaling analysis of micellar size has resulted from such an analogy.[11] To provide a basis for interpretation of our scattering measurements, we expand on this idea and describe a model of polymeric micelles based on the structure of a star-shaped polymer.[10,12,13] The recent development of synthetic star-shaped polymers led to a number of experimental studies[14-19] supplementing numerous theoretical[12,13,20] and computational[10] works. A star molecule exhibits a radial density profile characteristic of a semidilute polymer solution confined to a spherical domain. The star can be modeled as a collection of strings of blobs where within each blob the chain undergoes a self-avoiding walk.[21] The blob size increases with distance from the center of the star, producing a characteristic scaling behavior for the density profile. We model a micelle as a dense core of insoluble blocks and dispersed solvent surrounded by a corona with the characteristics of a star molecule.

An important feature of our micellar system is the ease with which we can dramatically alter the number of arms in our star-shaped aggregates. Since the presence of small quantities of water producs large changes in micelle dimension, we can provide a test of the star model over a wide range of arm lengths and number. Thus, if a star model holds for a micellar solution, such a system may expand the available experimental range providing a supplement to synthetic stars. In addition, a starlike micelle provides a much more physically reasonable picture than the uniform core-shell models previously employed.[7,22]

We first describe our static and dynamic light-scattering experiments including a description of data analysis procedures. We then present the results of those studies. We finally discuss the starlike model of a polymeric micelle and compare the scattering results to its predictions.

Experimental Section

Materials. Poly(ethylene oxide)/polystyrene diblock copolymer SE002, obtained from Polymer Laboratories Inc., was used without further purification. The block copolymer has a molecular weight of 187 500 g/mol, a polydispersity index M_w/M_n of 1.10, and ethylene oxide content of 4 wt %, based on GPC measurements of the polystyrene block and NMR experiments on the final block copolymer. Monodisperse polystyrene standards, with molecular weights and polydispersities listed in Table I, were purchased from Polysciences Inc. Cyclopentane (cp) from Eastman Kodak with a purity of 99% and reagent-grade toluene from J. T. Baker Chemical Co. were used without further purification. Distillation of the cyclopentane over sodium, performed in initial work with this system,[1] did not affect our results and therefore has been omitted. The water was treated in a Milli-Q unit.

Sample Preparation. Solutions of polystyrene (PS) homopolymer standards and poly(ethylene oxide)/polystyrene (PEO/PS) diblock copolymer were prepared in concentrations ranging from 0.1 to 5 mg/mL. Samples were filtered through Millipore Fluoropore 0.2-μm membrane filters into dust-free cylindrical light-scattering cells. Dilutions were made in the same cell by adding solvent filtered through 0.02-μm filters. Samples saturated with filtered water were shaken overnight and equil-

† Current address: Institute for Surface Chemistry, P.O. Box 5607, 114 86 Stockholm, Sweden.

0024-9297/91/2224-1670$02.50/0

Table I
Results for Dilute Solutions of Polystyrene Homopolymer at 23 °C

$M_w \times 10^{-5}$,[a] g/mol	M_w/M_n	cyclopentane $M_w \times 10^{-5}$, g/mol	cyclopentane $A_2 \times 10^5$, mL mol/g^2	toluene $M_w \times 10^{-5}$, g/mol	toluene $A_2 \times 10^5$, mL mol/g^2
4.0	1.06	4.07	2.0	4.47	54
2.6	1.06	2.74	2.3	2.67	51
1.6	1.10	1.70	2.8	1.76	45

[a] Values cited by Polysciences Inc.

ibrated for at least 24 h. Small water droplets were visible on the bottom of the scattering cells for these samples. Water content was determined by Karl Fischer titrations[1] with an Aquastar C2000 titrator and is reported in parts per million by weight (ppm). Concentrations (±3%) were determined after filtration by UV absorption at 260 nm.

Physical Properties. Solvent refractive indices of n_{tol} = 1.4915 (23 °C, 632.8 nm), n_{cp} = 1.4033 (23 °C, 632.8 nm), and n_{cp} = 1.4079 (23 °C, 514.5 nm) were obtained from the literature after corrections for temperature and wavelength dependences.[23] The specific refractive index increments (dn/dc) for PS and PEO/PS in cyclopentane were measured at 25 °C and 632.8 nm by using a KMX-16 laser differential refractometer, yielding $(dn/dc)_{PS}$ = 0.179 mL/g and $(dn/dc)_{PEO/PS}$ = 0.182 mL/g. We use a refractive index increment for polystyrene in toluene of 0.106 mL/g, also measured[24] at 632.8 nm. The temperature dependence of the refractive index increments for these solutions over narrow temperature intervals is negligible.[25] The cyclopentane viscosity of 0.432 cP was measured at 23 °C with a Cannon-Ubbelohde capillary viscometer. The physical properties needed for comparison with the star model, n_{PS} = 1.59, n_{PEO} = 1.46, n_{water} = 1.33, ρ_{PS} = 1.06 g/cm^3, and ρ_{PEO} = 1.13 g/cm^3 were obtained from the literature.[26]

Static Light Scattering. We modified a SOFICA 42000 photo-gonio-diffusometer[27] to operate with a 2-mW helium–neon laser instead of the original mercury lamp.[24] We removed all of the optical components previously positioned between the lamp and the vat window. The laser beam first passes through a beam splitter, sending 10% of the beam to a reference photomultiplier tube (PMT) to compensate for variations in the light source intensity. A mirror then directs the main beam through a diaphragm, to remove stray light, and neutral density filters, to attenuate the beam, before it enters the vat. The resulting incident beam is a collimated source of vertically polarized light with a wavelength of 632.8 nm.

The detector optical geometry has not been changed. Both reference and measuring PMTs have been replaced with Hamamatsu 1P28A PMTs, particularly sensitive to longer wavelengths. We fill the vat surrounding the sample cell with an index matching hydrocarbon mixture (n = 1.4512 at 23 °C and 632.8 nm) purchased from R. P. Cargille Laboratories Inc. Dust is removed by pumping the fluid through a 0.2-μm MF-Millipore filter hooked to the vat drain and the thermometer well. The vat is temperature controlled to ±0.05 °C with a circulating water bath.

Alignment was verified by measuring intensities from an isotropic scatterer (toluene) and comparing values of $I(\theta)\sin\theta$; deviations from unity remained below 2%. In a typical experiment we measure the scattering intensities at 11 angles, ranging from θ = 30° to 150°. We cycle through the angles three times and calculate mean values for each angle. A set of four to six samples with declining concentrations is used for each Zimm plot. Measurements of a toluene standard after each sample confirmed the spectrometer stability.

Dynamic Light Scattering. We use a Brookhaven Instruments BI-200 goniometer equipped with a Lexel Model 95 2-W argon ion laser at a wavelength of 514.5 nm to measure the hydrodynamic sizes of our micelles. The sample cell is surrounded with the index matching fluid described above. Temperature is controlled to ±0.05 °C by a water bath. Digital signals from the goniometer are processed by using a Brookhaven Instruments BI2030 136-channel correlator.

Data Analysis

Static Light-Scattering Measurements. Absolute intensity is often expressed in terms of the Rayleigh ratio:

$$R(\theta,c) = \frac{I(\theta,c)r^2}{I_0 V} \tag{1}$$

where $I(\theta,c)$ is the irradiance at a distance r of the light scattered from a solution with scattering volume, V, and I_0 is the irradiance of the incident light. The scattering angle, θ, is formed between the directions of the incident and detected light. The excess Rayleigh ratio, $\Delta R \equiv (R_{solution} - R_{solvent})$, from a dilute polymer solution is related to the weight-average molecular weight, M_w, in the following form:[28]

$$\frac{Kc}{\Delta R} = \frac{1}{M_w P(\theta)} + 2A_2 c + 3A_3 c^2 + \dots \tag{2}$$

where c is the polymer concentration in units of weight/volume and, for vertically polarized incident light, $K \equiv 4\pi^2 n^2 (dn/dc)^2/\lambda^4 N_A$ is an optical constant[29] combining n, the refractive index of the solvent, (dn/dc), the specific refractive index increment, λ, the wavelength of light in vacuo, and N_A, Avogadro's number. The concentration dependence of the excess scattering is embodied in second and third virial coefficients, A_2 and A_3.

The particle structure factor, $P(\theta)$, describes the angular dependence of the scattered light and begins to deviate from unity as the particle radius of gyration, R_g, approaches the inverse of the scattering vector, $1/q$, where $q \equiv (4\pi n/\lambda)\sin(\theta/2)$ and

$$\frac{1}{P(q)} = 1 + \frac{q^2\langle R_g^2\rangle}{3} + \dots \tag{3}$$

For polydisperse polymers, $\langle R_g^2\rangle \equiv \sum M_i c_i R_{g,i}^2 / \sum M_i c_i$ is the z-average square of the radius of gyration.[30]

Combining the equations above, we obtain

$$\frac{Kc}{\Delta R} = \frac{1}{M_w}\left[1 + \frac{16\pi^2 n^2}{3\lambda^2}\langle R_g^2\rangle \sin^2\left(\frac{\theta}{2}\right)\right] + 2A_2 c \tag{4}$$

This equation provides the basis for a Zimm plot,[31] where $Kc/\Delta R$ is plotted as a function of $\sin^2(\theta/2) + kc$ and k is an arbitrary constant, usually of order $\pm c^{-1}$, chosen to distribute points along the x axis. The initial slope of the curve comprising points extrapolated to $c = 0$ is proportional to $\langle R_g^2\rangle$, whereas the initial slope of the curve comprising points extrapolated to $\theta = 0$ is proportional to A_2. Extrapolation to both $c = 0$ and $\theta = 0$ yields an intercept inversely proportional to the weight-average molecular weight.

The micellar molecular weight can be determined directly if the system under study can be described by the model of closed association. This approach, introduced by Debye,[32] is valid at concentrations in the vicinity of the critical micelle concentration (cmc). The excess Rayleigh ratio contains the amount of scattering in addition to that from an "effective solvent", including the solvent and single chains at the critical micelle concentration:

$$\frac{K(c - \text{cmc})}{R - R_{cmc}} = \frac{1}{M_w P(\theta)} + 2A_2(c - \text{cmc}) + \dots \tag{5}$$

At concentrations much higher than the cmc, the measured intensity is dominated by the micelle contribution and the single chains can be neglected.

In some instances, the micellar molecular weight may be changing too rapidly to allow meaningful Zimm plot extrapolations to infinite dilution. However, evaluation

of the scattering angular dependence at each concentration will yield an apparent radius of gyration and molecular weight. The first means to obtain this information is equivalent to analyzing the angular dependence in the Zimm plot, where $Kc/\Delta R$ is plotted against $\sin^2(\theta/2)$. An alternate method utilizes the Guinier approximation for the form factor, $P(\theta) \equiv \exp(-q^2R_g^2/3)$ (ref 33) and involves a plot of ln $(\Delta R/Kc)$ versus $\sin^2(\theta/2)$. The behavior of these concentration-dependent parameters upon sample dilution will encompass both viral-type interactions as well as variations in micelle aggregation number. In the limit of infinite dilution, both methods should yield equivalent radii of gyration and weight-averaged molecular weights; we present results of both approaches for completeness.

Static light-scattering measurement of block copolymers is complicated by the fact that, in general, block copolymers are polydisperse in composition and molecular weight. For example, the weight-average molecular weight[34]

$$M_w = \frac{\sum c_i M_i (dn/dc)_i^2}{\sum c_i (dn/dc)_i^2} \quad (6)$$

depends on the potentially variable contrast between copolymer chains and the solvent, resulting in measurement of an *apparent* molecular weight. This problem is eliminated if the blocks have equal index of refraction increments, if one block is index-matched with the solvent, or if the sample is perfectly monodisperse in composition and molecular weight. In this study the block copolymer is highly asymmetric, consisting of 96% polystyrene by weight. The scattering is dominated by the polystyrene/cyclopentane contrast, evident by the similarity between the refractive index increments of the homopolymer (0.179 mL/g) and the block copolymer (0.182 mL/g). Therefore, the measured molecular weight should be very close to the true weight-average molecular weight.

To determine molecular weight, we need to measure intensity on an absolute scale. We calibrate the spectrophotometer with the Rayleigh ratio for toluene, $R_{tol}(\pi/2) = 1.402 \times 10^{-5}$ cm^{-1}, measured at 23 °C with vertically polarized laser light at 632.8 nm by Kaye and McDaniel.[35] We use

$$R(\theta) = I(\theta) \sin\theta \frac{R_{tol}(\pi/2)}{I_{tol}(\pi/2)} \left(\frac{n}{n_{tol}}\right)^2 \quad (7)$$

to convert the unpolarized intensity measured in a cylindrical cell, I, to the corresponding Rayleigh ratio. The scattering volume, determined by the intersection of the incident beam and the detected light, varies with scattering angle and is responsible for the correction factor $\sin\theta$. The last ratio is a refraction correction[27] for differences in scattering volume viewed by the detector. The design of the Sofica detection optics eliminates the need for reflection corrections.[36]

Dynamic Light-Scattering Measurements. We invert the correlation functions measured in dynamic light-scattering experiments with the data analysis program CONTIN,[37] developed by Provencher. CONTIN provides the smoothest nonnegative hydrodynamic size distribution that is consistant with the data. To reduce possible distortions due to oversmoothing, we decrease the importance of the curvature penalty term by setting the "probability one to reject" to 0.2, less smoothing than suggested by Provencher. We then compare several data sets (on the order of 10) at each angle to access the reliability of the resultant distributions. Details of the data analysis are discussed in a recent publication.[1]

We measure gradient diffusion coefficients of the micelles as a function of concentration and extrapolate to infinite dilution using $D = D_0(1 + K_D\phi)$, where K_D includes both thermodynamic and hydrodynamic interactions and ϕ is the volume fraction of the solute. In the limit of infinite dilution, the gradient diffusion coefficient is equal to the self-diffusion coefficient, and we can use the Stokes–Einstein relation to obtain hydrodynamic radii, $R_h = k_BT/6\pi\eta D_0$, where k_B is the Boltzmann constant, T the absolute temperature, and η the viscosity of the solvent.

Results

Polystyrene Solutions. We performed initial experiments with polystyrene standards to test the spectrophotometer. Table I summarizes the molecular weights and second virial coefficients obtained in toluene and cyclopentane, good and near-Θ-solvents, respectively, at 23 °C. The molecular weights agree within experimental error with those given by the manufacturer. The second virial coefficients are comparable to those found in the literature. We find $A_2 = 4.5 \times 10^{-4}$–5.4×10^{-4} mL mol/g^2 for polystyrene in toluene at 23 °C, whereas Appelt and Meyerhoff[38] report values of 1.35×10^{-4}–2.35×10^{-4} mL mol/g^2 at 20 °C, and Kniewske and Kulicke[39] report 1.4×10^{-4}–5.9×10^{-4} mL mol/g^2 at 25 °C. As expected, we find smaller positive second virial coeffients in cyclopentane, with values between 2.3×10^{-5} and 2.8×10^{-5} mL mol/g^2. A fit through the data of Berry et al.[40] suggests a somewhat smaller value of 1.6×10^{-5} mL mol/g^2.

We measured second virial coefficients for the 400 000 molecular weight PS homopolymer at temperatures ranging from 23 to 29 °C. The Θ temperature of 21.7 ± 0.5 °C was obtained by extrapolation of A_2 as a function of $1/T$ to $A_2 = 0$. Others have reported Θ temperatures for polystyrene in cyclopentane ranging from 19.6 to 23 °C.[40-43] It has been discussed, to some extent, that trace amounts of impurities can affect the Θ temperature.[44] This may explain the scatter in Θ temperature from different studies as cyclopentane from various sources can contain up to 5% linear alkanes. We were particularly interested in the effect of saturating amounts of water on the thermodynamic state of polystyrene in cyclopentane; however, as we increased the water content from ambient levels, 30–40 ppm, to the saturation level of 82–92 ppm, we found no detectable changes in the second virial coefficient.

Micellar Solutions. An earlier dynamic light-scattering study[1] revealed that the aggregation behavior of PEO/PS in cyclopentane is very sensitive to trace amounts of water. An increase in water content from 30 to 100 ppm can cause an increase in R_h on the order of 30–40%. We have also observed a surprising increase in micelle R_h upon dilution of solutions saturated with water, occurring below concentrations of 1×10^{-3} g/mL (see Figure 1). We initiated this static light-scattering study to investigate how micelle radii of gyration and aggregation numbers are affected by changes in water and copolymer concentrations. In particular, we would like to compare the structures formed in relatively dry micellar solutions with those saturated with water.

Solutions saturated with water have well-defined concentrations, with this polymer dispersing 0.7 molecule of water/ethylene oxide unit.[1] Solutions well below their saturation points, however, are difficult to prepare while maintaining a constant water content in the micelles. In these solutions we use the hydrodynamic size as an indication of solution conditions. We consider solutions having constant hydrodynamic sizes to have relatively constant solution conditions. We investigate such solu-

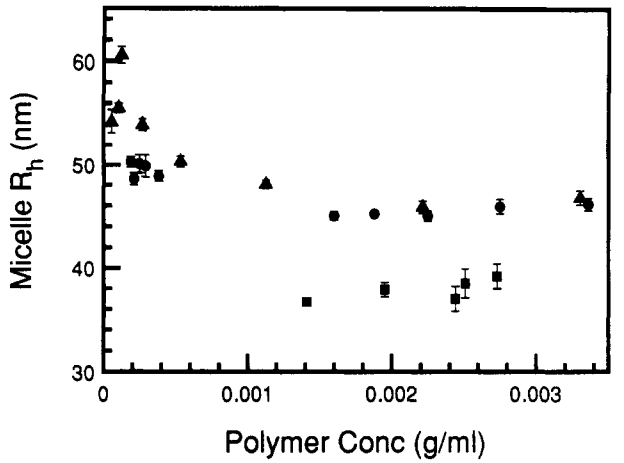

Figure 1. Micelle hydrodynamic radius as a function of copolymer concentration for solutions with 30–40 ppm water (■) and solutions saturated with water from this study (●) and a previous publication (▲).

tions of unsaturated micelles with 30–40 ppm of water for comparison with micelles saturated with water and refrain from interpreting small changes in size or thermodynamic properties. The sensitivity of these micelles to water content precludes virial analyses except when the solutions are saturated with water and can be diluted under conditions of constant water activity.

The critical micelle concentration (cmc) and hence the background concentration of single chains, decreases with the addition of water.[1] In solutions saturated with water the critical micelle concentration is too small to be detected, and thus single chains do not contribute to light-scattering signals and pose no ambiguity in data interpretation. In solutions having a low water content, unassociated chains can account for a substantial fraction of the scattered intensity. Using the approach of Debye,[32] subtracting the scattering and concentration due to single chains, we find cmc ranging from 8×10^{-5} to 5×10^{-4} g/mL; again, this is very sensitive to water content. Therefore light scattering from unsaturated solutions can include substantial contributions from single chains and should be analyzed with eq 5.

To apply the Zimm methodology, we desired regions where we could make sets of solutions of varying micellar concentration with micelles of constant size. We focus our attention on three concentration regimes, one having a low water content, 30–40 ppm, and two others saturated with water. The hydrodynamic radii in these three regions are shown in Figure 1, along with data from our previous publication.[1] Solutions with copolymer concentrations of 1.6×10^{-3}–3.4×10^{-3} g/mL have relatively constant micelle sizes with R_h of 34.9 nm for low water contents (30–40 ppm) and 43.9 nm at the saturation level (~100 ppm). These hydrodynamic values represent extrapolations to zero concentration; there is a slight virial behavior described below. These solutions are typical of our unsaturated and saturated micellar systems, and since they have fairly weak concentration dependences we can pursue a Zimm analysis of their size and mass as shown in Figure 2. Evaluation of dry solutions via Zimm analysis yields a weight-average aggregation number of 11; this value increases to 17 when corrected for the presence of single chains via either the Debye analysis or subtraction of cmc from the weight average. Zimm analysis of static light scattering from saturated solutions reveals a substantial increase in aggregation number, to 77, accompanying the increase in hydrodynamic size upon addition of water.

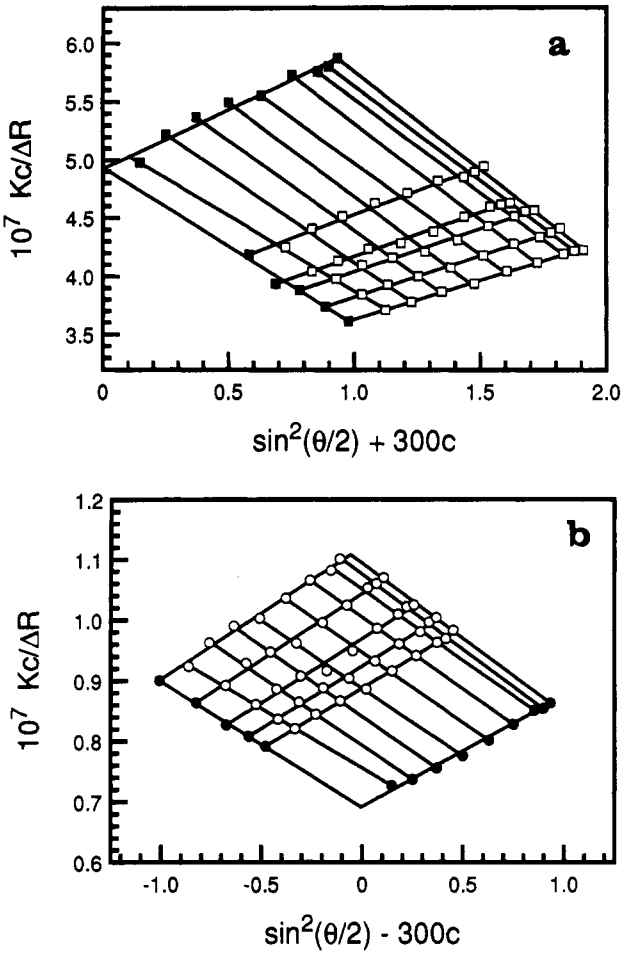

Figure 2. Zimm plots for solutions with (a) (□) 30–40 ppm water and 1.9×10^{-3}–3.2×10^{-3} g/mL of copolymer and (b) (○) saturation levels of water, 80–100 ppm, and 1.6×10^{-3}–3.4×10^{-3} g/mL of copolymer. Solid symbols indicate extrapolated values.

In general, second virial coefficients from associating solutions can be difficult to interpret. The concentration dependence of the saturated intensity should include individual terms for single chains and micelles as well as cross terms. Others[45] have found negative second virial coefficients in the vicinity of the cmc, where single chains make a significant contribution. We find a value of -2.0×10^{-5} mL mol/g^2 from the Zimm plot in Figure 2a for the low water content, 10^{-3} g/mL copolymer concentration regime. This negative virial coefficient could result from attractions between poorly shielded micellar cores; however, this behavior may also reflect a significant contribution from associating single chains. Since our solutions saturated with water are well beyond the cmc, we assume the concentration dependence to represent primarily micelle–micelle interactions. Here the second virial coefficient changes sign, with a value of 3.1×10^{-6} mL mol/g^2 in the saturated solutions at 10^{-3} g/mL copolymer. We envision the attractions between micellar cores to be better mediated by the solvated coronae; micelles saturated with water have higher aggregation numbers and denser coronae providing a more effective repulsive barrier between micellar cores.

We note that the latter second virial coefficient is smaller than the values we measured for homopolymer polystyrene in cyclopentane. Others have found smaller values of A_2 for star polymers when compared to values for linear chains, a trend in accord with predictions from the random-flight model.[46]

The virial behavior of the diffusion coefficient in solutions saturated with water reveals a slight retardation

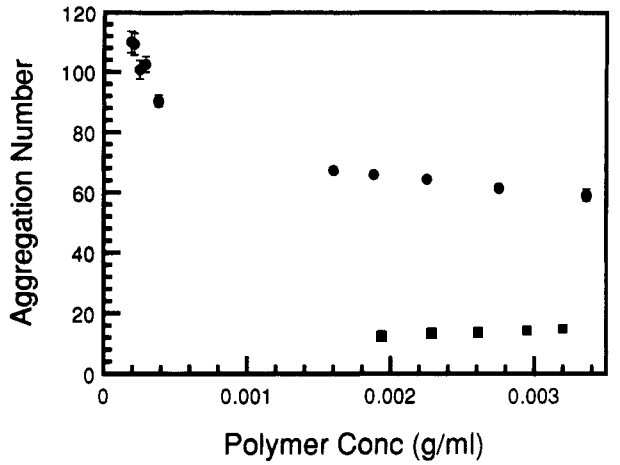

Figure 3. Apparent aggregation numbers for solutions (●) saturated with water and (■) below the saturation level (30–40 ppm).

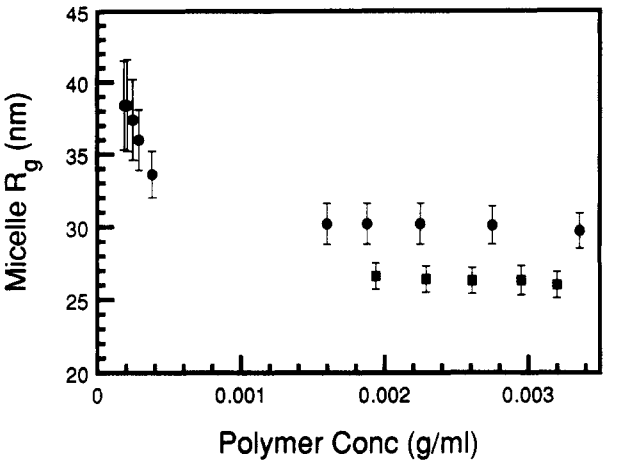

Figure 4. Apparent radii of gyration for (●) saturated and (■) unsaturated solutions. Error bars indicate agreement between values from angular dependence analysis of Zimm and Guinier plots.

of mutual diffusion with the coefficient K_D equal to −0.95. This coefficient can be attributed to thermodynamic and hydrodynamic interactions through the second virial coefficient and the virial coefficient for sedimentation via $K_D = 2A_2' + K_S$, where $A_2' = 3A_2M_M/N_A4\pi R_M^3$, R_M is the micelle radius, and M_M is the micellar molecular weight. Converting our results to these volume fraction units, using $R_h = R_M$, we find $A_2' = 3.03$, $K_D = -0.95$, and $K_s = -7.01$. These can be compared to the hard-sphere values, $A_2' = 4$, $K_D = 1.45$, and $K_s = -6.55$.[47,48] The increase in the magnitude of K_s over the hard-sphere value is typical of particles interacting via short-range attractions with repulsions of finite range as in an adhesive excluded shell potential.[48] An additional way to interpret these results is by analyzing the second virial coefficient in terms of a thermodynamic radius, $R_T^3 = 4\pi A_2M_M^2/3$. This provides a ratio of thermodynamic to hydrodynamic size, $R_T/R_h = 0.9$, reflecting greater thermodynamic penetrability in the outside of these micelles than in hard spheres.[15] In this regime, $R_T/R_h > 0.72$, homopolymer chains would have a positive K_D, indicating differences in both structure and interactions between these micelles and normal polymer coils.[23]

Upon dilution by a factor of 10, micelles saturated with water enlarge to have hydrodynamic radii of approximately 50 nm. In these very dilute solutions of saturated micelles, the aggregation numbers change too rapidly to enable meaningful Zimm plot extrapolations. Alternatively, we obtain concentration-dependent aggregation numbers by analyzing the angular dependence of the scattered light with Zimm plots and Guinier plots (described above). In Figure 3 we illustrate the dependence of micelle aggregation number on water and copolymer concentration by displaying averages at each concentration from a Guinier plot and the angular dependence of a Zimm plot for all three solution regimes. We find a 30% increase in aggregation number, to values on the order of 100, as solutions saturated with water are diluted by a factor of 10. Tuzar and co-workers have observed similar increases in aggregation number and hydrodynamic size when diluting micelles of fractionated triblock copolymers.[49]

Measured radii of gyration should reflect only micellar contributions because of the small size of the single chains compared to the probing radiation wavelength. Averages of the concentration dependent R_g's are shown in Figure 4 for all three solution regimes. At the higher concentrations, radii of gyration extrapolated to zero concentration increase from 27.4 to 30.8 nm as water concentrations are increased from 30–40 ppm to the saturation level. We find a further increase to values on the order of 37 nm upon dilution of micelles saturated with water.

Table II
Light-Scattering Results for PEO/PS = 170/1730 at 23 °C

PEO/PS conc, g/mL	$\sim 10^{-3}$	$\sim 10^{-3}$	2.5×10^{-4}
water conc, ppm	30–40	satd	satd
aggn no. (Zimm)	17	77	
aggn no. (Zimm, Ang)	17	77	103
aggn no. (Guinier)	17	76	98
A_2, mL mol/g^2	-2.0×10^{-5}	3.1×10^{-6}	
R_g, nm (Zimm)	27.9	31.7	
R_g, nm (Zimm, Ang)	28.1	32.0	39.4
R_g, nm (Guinier)	26.9	29.6	35.4
R_h, nm	34.9	43.9	50.1

We summarize our light-scattering measurements in Table II, where we present results from full Zimm plots, Zimm plot analysis of angular dependence, and Guinier plots. Values extrapolated to $c = 0$ are given for the two regimes at higher concentrations, whereas values for a representative solution are listed for the very dilute saturated micelles; again, neither a Zimm plot nor an extrapolation to infinite dilution is appropriate for the latter case because of the rapidly changing micelle size.

Discussion

The similarity of block copolymer micelles to star-shaped molecules has been realized for some time.[10–13] A star molecule having many branches or arms can be modeled as a collection of strings of blobs.[10] Within each blob the chain undergoes a self-avoiding walk, and the blob size increases as the string extends radially. Such a collection of blobs produces a density profile decaying with distance from the center, and thus chains are more swollen near the outside of the star than in the center.

We have developed a model of a micelle comprising a solid core of insoluble blocks and dispersed solvent surrounded by a shell or corona having the characteristics of a star polymer. This model allows us to further interpret the aggregation number, radius of gyration, and hydrodynamic size from light-scattering measurements.

The basis of our model is the radial density distribution of polymer segments within a many-arm star, $\rho(r) \propto f^{(3\nu-1)/2\nu}r^{(1-3\nu)/\nu}$, which varies with the number of arms, f, according to the exponent $\nu = {}^3/_5$ for a good solvent or ${}^1/_2$ near Θ conditions. Thus our model of the segment density profile within a micelle becomes

$$\rho(r) = \rho_c \quad r < R_c$$

$$\rho(r) = A(r/a_s)^{1/\nu}r^{-3} \quad R_c < r < R_m$$

$$\rho(r) = 0 \quad R_m < r \tag{8}$$

where R_c is the core radius, R_m the micelle radius, and a_s is the size of the monomers in the corona or shell. The core density, ρ_c, represents the density of the core polymer alone or with dispersed solvent, and A is a constant to be determined below. We denote $\xi(r)$, the diameter of a blob, and require that in the first layer of f blobs, $\xi(R_c)$ be defined such that the surface area match that of the core, providing

$$\xi(R_c) = 4R_c/f^{1/2} \tag{9}$$

a relationship between the blob size at the core–corona boundary and the core size and aggregation number. Since there are $(\xi/a_s)^{1/\nu}$ monomers/blob, we can match the density at the core–corona boundary

$$\rho(R_c) = \frac{3\cdot 4^{1/\nu}(R_c/a_s)^{1/\nu}f^{(3\nu-1)/2\nu}}{32\pi R_c^{\,3}} = A(R_c/a_s)^{1/\nu}R_c^{-3} \tag{10}$$

to determine the constant of proportionality $A = 3\cdot 4^{1/\nu}f^{(3\nu-1)/2\nu}/32\pi$.

This model density distribution can be used to determine the radius of gyration as a function of the micelle size, aggregation number, core size, and the scattering contrast of the two blocks.[9] If one assumes that micelles are poorly draining, one can equate the hydrodynamic radius with the micelle radius to determine R_g. We apply a more stringent test and predict both the overall radius and radius of gyration from the aggregation number determined from our scattering measurements. Thus we relate the micelle size and core dimension to the aggregation by requiring integration over the micelle density profile to recover the total number of monomers:

$$\int \rho(r)\, dV = Nf \tag{11}$$

In the core, this produces the familiar packing constraint

$$R_c = \left(\frac{3N_c f}{4\pi\rho_c}\right)^{1/3} \tag{12}$$

while integration over the corona results in

$$R_m = \left(\frac{8N_s f^{(1-\nu)/2\nu}}{3\cdot 4^{1/\nu}\nu}a_s^{\,1/\nu} + R_c^{\,1/\nu}\right)^{\nu} \tag{13}$$

a relationship between the micelle size, aggregation number and core dimension.

Finally, we determine the radius of gyration measured from light scattering by integrating the second moment of the refractive index profile:

$$\langle R_g^{\,2}\rangle = \int_0^\infty n(r)r^4\, dr / \int_0^\infty n(r)r^2\, dr \tag{14}$$

with

$$n(r) = (n_c - n_0) \quad r < R_c$$

$$n(r) = (n_s - n_0)AV_s(r/a_s)^{1/\nu}r^{-3} \quad R_c < r < R_m$$

$$n(r) = 0 \quad R_m < r$$

where $n_s - n_0$ and $n_c - n_0$ are the differences between the refractive indexes of the shell and solvent and the core and solvent, respectively. On the basis of the Gladstone–Dale equation[50] for the refractive index increment, we weight the index of refraction difference by the local polymer volume fraction, multiplying the number density by the volume per statistical segment, V_s.

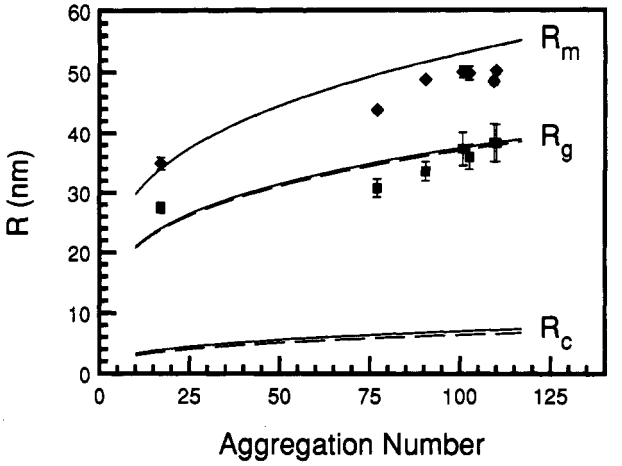

Figure 5. Comparison of experimental sizes, (■) radii of gyration, and (◆) hydrodynamic radii, with starlike micelle model predictions, where R_m, R_g, and R_c are micelle radii, radii of gyration, and core radii, respectively. Dashed lines and solid lines illustrate small variations for the system under study with no water and saturation levels of water, respectively.

To model poly(ethylene oxide)/polystyrene in cyclopentane we choose the exponent $\nu = {}^1/_2$ representative of the near-Θ condition of the styrene chains; we use the indexes of refraction and densities described above. We define the statistical segment length as $a_s^2 = 6R_g^2/N_s$ and determine from the data of Berry[51] that polystyrene in cyclohexane at Θ conditions has $a_s = 1.55$ nm, equivalent to 5 monomers/statistical segment. Thus, while N_c represents the number of monomers per insoluble block, N_s specifies the number of statistical segments per soluble block.

We demonstrate the effect of aggregation number on our calculated radius and radius of gyration in Figure 5. We note that the micellar size increases slowly with aggregation number due to the efficient packing of chains in a star configuration.

When these block copolymer micelles are saturated with water, there is 0.7 molecule of water/ethylene oxide repeat unit. Under these conditions we use a volume-average index of refraction to describe the PEO and water assumed to be homogeneously distributed throughout the core. The addition of water to the core of the micelle increases the core diameter but has little discernible effect on the overall micelle size as shown in Figure 5. The primary effect of saturation with water is the dramatic increase in the aggregation number, shifting the radius of gyration and overall radius solely by the addition of chains to the micelle.

We compare the model predictions of R_g and R_m with our measurements of R_g and R_h in Figure 5 and Table III. Clearly, the model best predicts radius of gyration when depicting saturated micelles with aggregation numbers from 77 to 100. The agreement is reasonable for both hydrodynamic and gyration radii, although the slight overprediction of R_h suggests that there is some draining in the outer portions of the starlike micelles.

The radius of gyration prediction for micelles at low water content errs, falling below the measured value. Several factors may contribute to this discrepancy including uncertainties in the model parameters such as segment size and density. Perhaps more important is the

Table III
Comparison of Experimental Values and Starlike Micelle Predictions

PEO/PS conc, g/mL	$\sim 10^{-3}$	$\sim 10^{-3}$	2.5×10^{-4}
water conc, ppm	30–40	satd	satd
aggn no.	17	77	100
	Experimental Values		
R_g, nm	27.5	30.8	37.4
R_h, nm	34.9	43.9	49.6
R_g/R_h	0.79	0.70	0.75
	Starlike Micelles		
R_g, nm	24.0	35.4	37.8
R_m, nm	34.0	49.7	53.1
R_g/R_h	0.71	0.71	0.71
R_c, nm	3.5	6.4	7.0
$\xi(R_m)$, nm	33.0	22.7	21.2

failure of the scaling model for stars with fewer than 30 arms;[10] in particular, for small numbers of arms there is a crossover between $\langle R_g^2 \rangle$ scaling as Nf for $f = 1, 2$ to $Nf^{1/2}$ for many arms. When there are too few chains in a micelle, the arms in the corona are not stretched into the string of blobs supposed in the star model. In fact, the outer region of a micelle having fewer than 20 arms may not even be at semidilute conditions. We can characterize the applicability of the starlike micelle model by evaluating the blob size at the micelle boundary, $\xi(R_m)$. This blob size can be compared to the size of the polystyrene arm if it were detached and existed as a Gaussian coil, $\xi_{coil} = a_s N_s^{1/2} = 29$ nm. We see in Table III that only the saturated micelles have outer blob dimensions smaller than the unperturbed arm dimensions. The blob size on the outside of a micelle begins to exceed the polymer coil size when there are 30 chains/micelle, the same point where the scaling behavior begins to deviate from simulation results.[10]

The micelles with low water content and an aggregation number of 17 show $R_g/R_h = 0.80$, a ratio consistent with similar star molecules at Θ conditions shown in Figure 6; 18-arm stars have $R_g/R_h = 0.85$, while with 12-arm stars, $R_g/R_h = 0.89$.[14,52] This can be contrasted with $R_g/R_h = 1.24$ calculated from renormalization group theory for a nondraining Gaussian chain.[53] Burchard and co-workers have predicted values of R_g/R_h for several polymer architectures, ranging from 1.50 for unperturbed linear chains to 1.08 for unperturbed stars with many arms.[54] Although their predictions qualitatively display the decreasing R_g/R_h with arm number seen experimentally with micelles and stars of relatively few arms, the values are substantially overpredicted. Nevertheless, the fact that R_g/R_h increases with decreasing number of arms suggests that the micelles having fewer chains will approach single-chain behavior, and only above a threshold aggregation number can one expect star behavior.

The ratio of the radius of gyration to the micelle radius from the starlike micelle model is approximately 0.71, increasing slightly as more chains are added to the micelle. A star molecule having no core has a ratio of R_g to R_m equal to $(1 + 2\nu)^{-1/2}$, or 0.707 in Θ conditions. Thus, due to its small core, our starlike micelle is very similar to a true star. Experimentally, we find the saturated micelles of 77 chains to have a radius of gyration to hydrodynamic radius of 0.70, very close to our model predictions if we assume nondraining coronae, as shown in Table III. At lower concentrations the micelles contain approximately 100 chains and exhibit larger $R_g/R_h = 0.75$, a value between a solid sphere [=0.775] and a nondraining star.

One would expect R_g/R_h to be less than the hard-sphere value for compact particles with radially decreasing segment densities. Ratios as low as 0.6 have been observed for heterogeneously swollen microgels.[55] In the case of block copolymer micelles, the starlike micelle model provides a convincing explanation for a minimum in the variation of the R_g/R_h as a function of aggregation number.

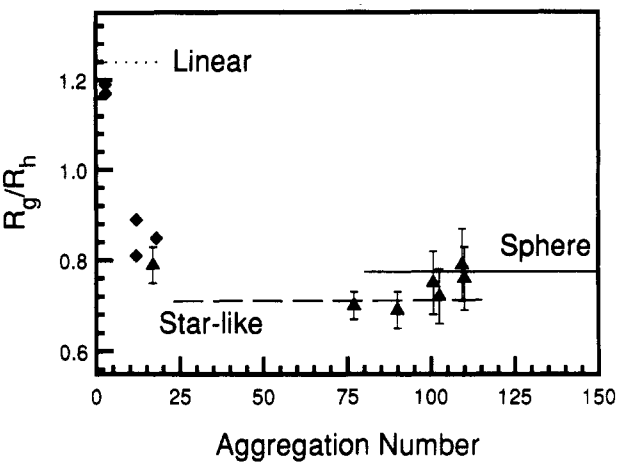

Figure 6. Variations in ratios of radius of gyration over hydrodynamic radius as a function of aggregation number, where (▲) are values from this study and (◆) are values for polystyrene star molecules at Θ conditions (data taken from refs 14 and 52). Comparisons are made with limiting values for a linear chain at Θ conditions and a homogeneous sphere. Comparisons with starlike micelle model approximates R_h as R_m.

Conclusions

We have shown light-scattering measurements revealing that poly(ethylene oxide)/polystyrene block copolymers in cyclopentane undergo remarkable increases in aggregation number upon saturation with water, from 17 to 77 chains per micelle. This micellar molecular weight increase is accompanied by an increase in the hydrodynamic and gyration radii. We find that solutions having relatively low water content have appreciable single chains present and require careful interpretation of light-scattering data. Micellar solutions saturated with water have insignificant concentrations of single chains and can be diluted at constant water activity. The concentration dependence in these water-saturated micelles reflects soft-sphere interaction in both the second virial coefficient and the concentration dependence of the diffusion coefficient. At very low concentrations, saturated micelles enlarge upon dilution; estimates of the aggregation number for a solution typical of this regime indicate 100 chains/micelle.

We interpret our scattering results in the context of a starlike micelle model. These structures comprise a solid core of insoluble blocks plus dispersed solvent surrounded by a corona exhibiting the concentration profile expected for star-shaped polymers. We find from our results that the starlike micelle describes the radius of gyration and hydrodynamic radius of our micelles quite well. This model only begins to fail as the aggregation number becomes small. We expect the starlike micelle model to be valid for aggregation numbers exceeding 30; below this aggregation number, the chains are no longer in a semidilute micelle. We also present the ratio of gyration to hydrodynamic radius and find behavior spanning a region between Gaussian chain behavior and hard spheres. Analysis of such a ratio provides an additional means to interpret micellar structure.

Acknowledgment. This work has been partially supported by the Center for Materials Research at Stanford University under the NSF-MRL program and the

General Electric Co. L.J.M.V.'s visit was supported by Du Pont Marshall Laboratories, and K.A.C. gratefully acknowledges the support of the Eastman Kodak Co. and AT&T Laboratories. We thank Frans Leermakers, Jennifer Raeder and Dave Hoagland for useful discussions regarding this work.

References and Notes

(1) Cogan, K. A.; Gast, A. P. *Macromolecules* **1990**, *23*, 745.
(2) Gallot, Y.; Leng, M.; Benoit, H.; Rempp, P. *J. Chim. Phys.* **1962**, *59*, 1093.
(3) Gallot, Y.; Franta, E.; Rempp, P.; Benoit, H. *J. Polym. Sci.: Part C* **1964**, *4*, 473.
(4) Riess, G.; Bahadur, P.; Hurtrez, G. *Encyclopedia of Polymer Science and Engineering*; Wiley: New York, 1985; Vol. 2, p 324.
(5) Tuzar, Z.; Kratochvil, P. *Adv. Colloid Interface Sci.* **1976**, *6*, 201.
(6) Marie, P.; Gallot, Y. *Makromol. Chem.* **1979**, *180*, 1611.
(7) Plestil, J.; Baldrian, J. *Makromol. Chem.* **1973**, *174*, 183.
(8) Oranli, L.; Bahadur, P.; Riess, G. *Can. J. Chem.* **1985**, *63*, 2691.
(9) Gast, A. P. *Scientific Methods for the Study of Polymer Colloids and Their Applications*; Ottewill, R. H., Ed.; NATO ASI Series C; Kluwer Academic: Netherlands, 1990; p 311.
(10) Grest, G. S.; Kremer, K.; Witten, T. A. *Macromolecules* **1987**, *20*, 1376.
(11) Halperin, A. *Macromolecules* **1987**, *20*, 2943.
(12) Witten, T. A.; Pincus, P. A. *Macromolecules* **1986**, *19*, 2509.
(13) Daoud, M.; Cotton, J. P. *J. Phys. (Paris)* **1982**, *43*, 531.
(14) Huber, K.; Burchard, W.; Fetters, L. J. *Macromolecules* **1984**, *17*, 541.
(15) Bauer, B. J.; Fetters, L. J.; Graessley, W. W.; Hadjichristidis, N.; Quack, G. F. *Macromolecules* **1989**, *22*, 2337.
(16) Lantman, C. W.; MacKnight, W. J.; Tassin, J. F.; Monnerie, L.; Fetters, L. J. *Macromolecules* **1990**, *23*, 836.
(17) Richter, D.; Stuhn, B.; Ewen, B.; Nerger, D. *Phys. Rev. Lett.* **1987**, *58*, 2462.
(18) Richter, D.; Farago, B.; Fetters, L. J.; Huang, J. S.; Ewen, B. *Macromolecules* **1990**, *23*, 1845.
(19) Dozier, W. D.; Huang, J. S.; Fetters, L. J. Submitted to *Macromolecules*.
(20) Benoit, H. *J. Polym. Sci.* **1953**, *11*, 507.
(21) de Gennes, P.-G. *Scaling Concepts in Polymer Physics*; Cornell University Press: Ithaca, NY, 1979.
(22) Whitmore, M. D.; Noolandi, J. *Macromolecules* **1988**, *21*, 1482.
(23) Johnson, B. L.; Smith, J. *Light Scattering from Polymer Solutions*; Huglin, M. B., Eds.; Academic Press: London, 1972; p 27.
(24) Millaud, B.; Strazielle, C. *Makromol. Chem.* **1979**, *180*, 441.
(25) Huglin, M. B. *Light Scattering from Polymer Solutions*; Huglin, M. B., Ed.; Academic Press: London, 1972; p 165.
(26) Brandrup, J., Immergut, E. H., Eds. *Polymer Handbook*, 3rd ed.; Wiley: New York, 1989.
(27) Societe Francaise d'Instruments de Controle et d'Analyses, *Instruction Manual for Sofica Photo-Gonio Diffusometer*, 1965.
(28) Zimm, B. H. *J. Chem. Phys.* **1948**, *16*, 1093.
(29) Carr, C. I.; Zimm, B. H. *J. Chem. Phys.* **1950**, *18*, 1616.
(30) Chu, B. *Determination of Molecular Weight*; Cooper, A. R., Ed.; Wiley: New York, 1989; p 53.
(31) Zimm, B. H. *J. Chem. Phys.* **1948**, *16*, 1099.
(32) Elias, H.-G. *Light Scattering from Polymer Solutions*; Huglin, M. B., Ed.; Academic Press: London, 1972; p 397.
(33) Guinier, A.; Fournet, G. *Small Angle Scattering of X-Rays*; Wiley: New York, 1955.
(34) Hilfiker, R.; Chu, B.; Xu, Z. *Colloid Interface Sci.* **1989**, *133*, 176.
(35) Kaye, W.; McDaniel, J. B. *Appl. Opt.* **1974**, *13*, 1934.
(36) Tomimatsu, Y.; Vitello, L.; Fong, K. *J. Colloid Interface Sci.* **1968**, *27*, 573.
(37) Provencher, S. W.; Hendix, J.; De Maeyer, L.; Paulussen, N. *J. Chem. Phys.* **1978**, *69*, 4273.
(38) Appelt, B.; Meyerhoff, G. *Macromolecules* **1980**, *13*, 657.
(39) Kniewske, R.; Kulicke, W.-M. *Makromol. Chem.* **1983**, *184*, 2173.
(40) Berry, G. C.; Casassa, E. F.; Liu, P.-Y. *J. Polym. Sci., Polym. Phys. Ed.* **1987**, *25*, 673.
(41) Deschamps, H.; Leger, L. *Macromolecules* **1986**, *19*, 2760.
(42) Brown, W. *Macromolecules* **1986**, *19*, 387.
(43) Munch, J.-P.; Hild, G.; Candau, S. *Macromolecules* **1983**, *16*, 71.
(44) Hu, H. W.; Van Alsten, J.; Granick, S. *Langmuir* **1989**, *5*, 270.
(45) Kotaka, T.; Tanaka, T.; Hattori, M.; Inagaki, H. *Macromolecules* **1978**, *11*, 138.
(46) Berry, G. C. *J. Polym. Sci. A-2* **1971**, *9*, 687.
(47) Berne, B. J.; Pecora, R. *Dynamic Light Scattering*; Wiley: New York, 1976.
(48) Russel, W. B.; Saville, D. A.; Schowalter, W. R. *Colloidal Dispersions*; Cambridge University Press: Cambridge, 1989.
(49) Tuzar, Z.; Stepanek, P.; Konak, C.; Kratochvil, P. *J. Colloid Interface Sci.* **1985**, *105*, 372.
(50) Kratochvil, P. *Classical Light Scattering From Polymer Solutions*; Elsevier: Amsterdam 1987.
(51) Berry, G. C. *J. Chem. Phys.* **1966**, *44*, 4550.
(52) Khasat, N.; Pennisi, R. W.; Hadjichristidis, N.; Fetters, L. J. *Macromolecules* **1988**, *21*, 1100.
(53) Oono, Y. *J. Chem. Phys.* **1983**, *79*, 4629.
(54) Burchard, W.; Schmidt, M.; Stockmayer, W. H. *Macromolecules* **1980**, *13*, 1265.
(55) Antonietti, M.; Bremser, W.; Schmidt, M. *Macromolecules* **1990**, *23*, 3796.